Nonstoichiometry studies of the Y-Ba-Cu-O system in terms of a real-space scattering coherent-potential approximation

L. Szunyogh
Institut für Technische Elektrochemie, Technische Universität Wien, Wien, Austria

G. H. Schadler
Laboratorium für Festkörperphysik, Eidgenössische Technische Hochschule Zürich, Switzerland

P. Weinberger
Institut für Technische Elektrochemie, Technische Universität Wien, Wien, Austria

R. Monnier
Laboratorium für Festkörperphysik, Eidgenossische Technische Hochschule Zürich, Switzerland

R. Podloucky
Institut für Physikalische Chemie, Universität Wien, Wien, Austria
(Received 10 July 1989)

A careful study of nonstoichiometry effects for the O(1), O(2), O(3), and O(4) constituents is performed using a real-space scattering cluster coherent-potential approximation method. By increasing successively the cluster size, a numerically optimal convergence of the effective scattering amplitudes can be obtained. In order to calculate spectral quantities such as the density of states (DOS) and componentlike DOS, these scattering amplitudes are then used for rather large clusters of up to 160 atoms. We find that a cluster size of about 70 atoms guarantees reliable effective scattering amplitudes. As an application the calculation of x-ray emission and x-ray photoemission spectra and of the spherical part of the Hopfield parameter as a function of nonstoichiometry is shown.

I. INTRODUCTION

The study of the relation between stoichiometry or composition and physical properties has been the main experimental tool in the quest for the mechanism leading to the high-temperature superconductivity. In $YBa_2Cu_3O_{7-\delta}$ T_c shows two distinct plateaus as a function of oxygen concentration, one at 90 K for $0 \leq \delta \leq 0.2$ and a second at 60 K for $0.3 \leq \delta \leq 0.5$.[1] A more recent systematic investigation[2] for compounds with Y partially substituted by Ca or Ba by La suggests that the relevant quantity to compare T_c with is the ionicity p of the Cu-O complexes in the two-dimensional sheets and a plot of T_c versus p shows the same two-plateau behavior as T_c versus δ in the original system.

Of the theoretical models in the field of high-T_c superconductivity, only those based on density-functional theory, i.e., band-structure or cluster calculations, can hope to eludicate the effects of ionic substitution or nonstoichiometry on the charge distribution. Although this approach is expected to fail when it comes to the description of excitation spectra of the copper oxide based compounds, the experimental situation is yet ambiguous enough to make a study of the *differences* in the x-ray photoemission spectra (XPS) and x-ray emission spectra (XES) as a function of composition worthwhile within that framework. More interesting still is the evolution of the electron-phonon interaction, monitored by the Hopfield parameter, with the oxygen content. Although the exchange of virtual phonons is probably not the dominant pairing mechanism in these (polar) compounds, one expects the electron-phonon coupling to be strong and to systematically depend on the doping.

In what follows, we shall apply the real-space cluster coherent potential approximation method to the study of the density of states (DOS), the XPS and XES, and the Hopfield parameter in $YBa_2Cu_3O_{7-\delta}$ for various stoichiometries.

II. THEORY

In this section we present a short summary of the real-space scattering cluster (RSSC) coherent-potential-approximation (CPA) formalism together with explicit formulas for the physical quantities of interest for our discussion. In multiple scattering theory for solids the central quantity to be calculated is the scattering path operator (SPO),[3,4]

$$\underline{\tau}(\varepsilon)=\{\tau^{ij}(\varepsilon)\} , \tag{1}$$

which is given for an ensemble of scatterers (cluster) by

$$\underline{\tau}(\varepsilon)=[\underline{t}^{-1}(\varepsilon)-\underline{G}(\varepsilon)]^{-1} , \tag{2}$$

where ε is the energy and the supermatrices $\underline{G}(\varepsilon)$ and $\underline{t}(\varepsilon)$ comprise the real-space structure constants and the single-site t matrices,[5] respectively:

 ©1990 The American Physical Society

$$\underline{G}(\varepsilon)=\{\mathbf{G}^{ij}(\varepsilon)\},\quad \mathbf{G}^{ij}(\varepsilon)=\{G^{ij}_{LL'}(\varepsilon)\},\quad L=(lm)\ , \tag{3}$$

$$\underline{t}^{-1}(\varepsilon)=\begin{Bmatrix} \ddots & & & \\ & \mathbf{t}_{i\alpha}^{-1}(\varepsilon) & 0 & \\ & & \ddots & \\ & 0 & & \mathbf{t}_{jX}^{-1}(\varepsilon) \\ & & & & \ddots \end{Bmatrix}. \tag{4}$$

The indices i and j denote sites and run from 1 to N, where N is the number of atoms in the cluster. In (1)–(4) bold symbols denote angular momentum representations (see, e.g., Ref. 5) and underlines, supermatrices. In (4) the case is indicated that one particular sublattice is statistically disordered by two components $\alpha=A,B$; i.e., position i is occupied, for example, by one type of oxygens or vacancies, while the other sublattices are ordered (X=Y, Ba, Cu, and the other oxygens).

If a particular subcell i of the disordered sublattice is occupied by species α, while all other sites in this sublattice are effective scatterers, the corresponding subcell-diagonal SPO is given by

$$[\underline{\tau}^{i\alpha}(\varepsilon)]_{ii}=[\{\mathbb{1}+\underline{\tau}_c(\varepsilon)[\underline{t}_{i\alpha}^{-1}(\varepsilon)-\underline{t}_c^{-1}(\varepsilon)]\}^{-1}\underline{\tau}_c(\varepsilon)]_{ii}\ , \tag{5}$$

$$\underline{t}_c^{-1}(\varepsilon)=\begin{Bmatrix} \ddots & & & \\ & \mathbf{t}_{ic}^{-1}(\varepsilon) & 0 & \\ & & \ddots & \\ & 0 & & \mathbf{t}_{jX}^{-1}(\varepsilon) \\ & & & & \ddots \end{Bmatrix}, \tag{6}$$

where the subscript c ("coherent") denotes the case that all sites of the disordered sublattice are occupied by effective scatterers. The (single-site) coherent-potential approximation (Refs. 3 and 4) is then given by the following condition:

$$c[\underline{\tau}^{iA}(\varepsilon)]_{ii}+(1-c)[\underline{\tau}^{iB}(\varepsilon)]_{ii}=[\underline{\tau}_c(\varepsilon)]_{ii}\ , \tag{7}$$

which, because of (2), has to be solved self-consistently and where c is the concentration of species A.

The partial local componentlike densities of states (LDOS's) $n_l^i(\varepsilon)$ in a chosen subcell i are then defined as

$$n_l^i(\varepsilon)=-\frac{2}{\pi}F_l^i(\varepsilon)\sum_m \mathrm{Im}[\underline{\tau}(\varepsilon)]_{ii;lm,lm}\ , \tag{8}$$

where the $F_l^i(\varepsilon)$ are radial normalization integrals restricted to the ith muffin tin[5] and the factor 2 takes into account trivial spin degeneracy.

In terms of these partial local componentlike DOS's the theoretical x-ray emission intensity spectra (XES) can be compared by using the well-known expression

$$I_l^{i\alpha}(\varepsilon)=\mathrm{const}(\Delta\varepsilon)^3\sum_{l'}\sigma_{l,l'}^{i\alpha,i\alpha}(\varepsilon,\varepsilon_f)n_{l'}^{i\alpha}(\varepsilon),\quad \alpha=A,B\ , \tag{9}$$

where ε_f is the energy of a core state corresponding to an angular momentum eigenvalue l and the $\sigma_{l,l'}^{i\alpha,i\alpha}(\varepsilon,\varepsilon_f)$ are the transition matrix elements.[6,7] It should be noted that XES is a site-specific spectroscopy; i.e., if i refers to a subcell of the disordered sublattice, this cell can therefore be occupied by either an A or B atom.

A formally similar expression can be used for the inten-

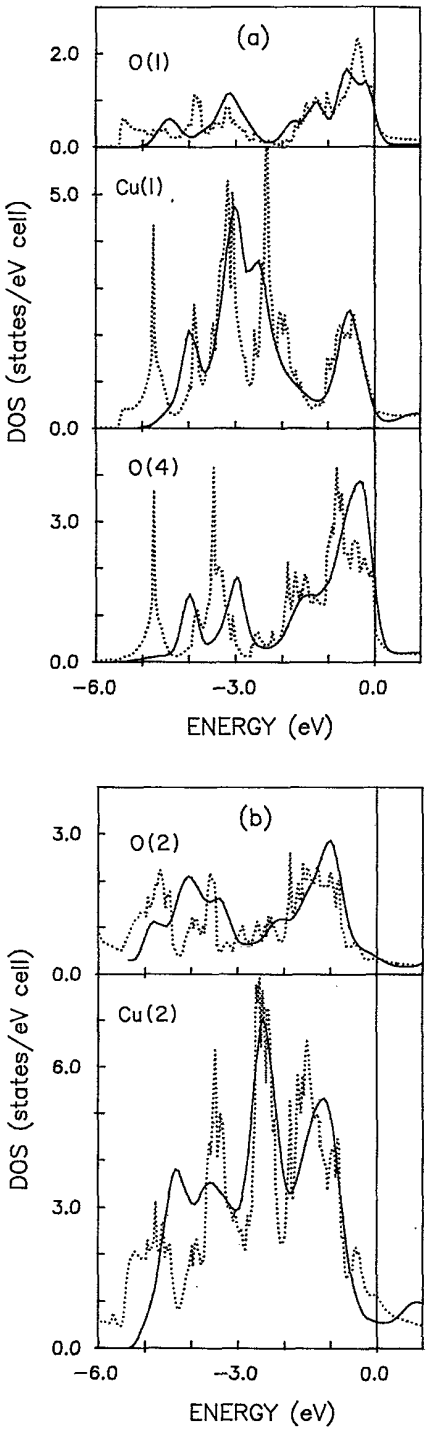

FIG. 1. (a) O(1) and O(4) p-like and Cu(1) d-like DOS and (b) O(2) p-like and Cu(2) d-like DOS for $YBa_2Cu_3O_7$. The zero of energy refers to the FLAPW (Ref. 13) Fermi level. Solid line: cluster calculation and dotted line: FLAPW (Ref. 13).

sity of x-ray photoemission spectra (XPS):[8,9]

$$\langle I^i(\varepsilon)\rangle = \text{const} \sum_{\alpha=A,B} c_\alpha \sum_l \sigma_l^{i\alpha;i\alpha}(\varepsilon,\varepsilon+\omega) n_l^{i\alpha}(\varepsilon) \ . \quad (10)$$

In (10) the $\sigma_l^{i\alpha,i\alpha}(\varepsilon,\varepsilon+\omega)$ are cross sections as calculated in terms of the single-scatterer final-state approximation and ω is the energy of the incident photon beam. Since photoemission spectra are not site specific, for subcells corresponding to the disordered sublattice the average over the components has to be taken.

The partial local componentlike DOS can also be used to calculate estimates of the electron-phonon enhancement. Within the rigid-muffin-tin approximation (RMTA) (Ref. 10) the spherical (McMillan-)Hopfield parameter is given by[11,12]

$$\eta_0^{i\alpha} = \frac{1}{n(\varepsilon_F)} \sum_{ll'} \begin{bmatrix} l & 1 & l' \\ 0 & 0 & 0 \end{bmatrix}^2 T_{l,l'}^{i\alpha,i\alpha}(\varepsilon_F)^2 n_l^{i\alpha}(\varepsilon_F) n_{l'}^{i\alpha}(\varepsilon_F) F_l^{i\alpha}(\varepsilon_F)^{-1} F_{l'}^{i\alpha}(\varepsilon_F)^{-1}, \quad \alpha = A,B \ , \quad (11)$$

where $n(\varepsilon_F)$ is the total DOS at the Fermi level and the

$$\begin{bmatrix} l & 1 & l' \\ 0 & 0 & 0 \end{bmatrix}$$

are $3j$ coefficients, which automatically provide the selection rules $l'=l\pm1$. The $T_{l,l'}^{i\alpha,i\alpha}(\varepsilon_F)$ are radial integrals [see, e.g., Eq. (12.15) of Ref. 5], where the integrand involves the radial gradient of the potential and the radial parts of the scattering solutions.

III. COMPUTATIONAL DETAILS

The calculations are performed using a muffin-tin-ized form of the full-potential linear augmented-plane-wave method (FLAPW) potential of Massidda *et al.*,[13] to which the vacancy potentials are matched by means of the Mattheis prescription, ignoring charge self-consistency. The CPA equations (2) and (6) are solved self-consistently parallel to the real axis using the numerical scheme proposed by Ginatempo and Staunton[14] and then deconvoluted by means of a numerical Riemann-Cauchy continuation to the real axis. In general, an energy mesh on the real axis of 0.01 Ry is used. However, in the narrow range below the Fermi energy ε_F, where a sharp peak in the O(1) and O(4) DOS was found in the FLAPW calculations,[13,15] a grid size of 0.01 eV is applied.

For the single-site averaged effective CPA scattering amplitudes we find that by increasing the cluster size up to 161 atoms, about 70 atoms are sufficient to guarantee convergence for the CPA solution. Therefore the results presented in the next section correspond to clusters containing about 70 atoms.

IV. RESULTS

In Figs. 1(a) and 1(b) we compare the partial local DOS (LDOS) obtained in our cluster calculation for the stoichiometric ($\delta=0$) compound with the FLAPW results of Massidda *et al.*[13] for the infinite crystal. The cluster approximation leads to much smoother curves, due to the absence of van Hove singularities and the use of complex energies. The overall agreement between the

TABLE I. Correction to the interstitial charge Δ, calculated Fermi energy ε_F, total DOS at the Fermi energy $n(\varepsilon_F)$, and total charge per site (Q_i) in $YBa_2Cu_3O_{7-\delta}$ for various vacancy concentrations δ. The column labeled CPA denotes the disordered sublattice.

CPA	δ	Δ	ε_F	$n(\varepsilon_F)$	Q_Y	Q_{Ba}	$Q_{Cu(1)}$	$Q_{O(1)}$	$Q_{Cu(2)}$	$Q_{O(2)}$	$Q_{O(3)}$	$Q_{O(4)}$	Q_{vac}
O(1)	0.0	2.11	0.4536	95.93	0.81	1.20	9.05	4.93	9.18	5.29	5.16	4.73	
	0.1		0.4533	94.00	0.81	1.19	9.07	4.99	9.18	5.29	5.16	4.73	0.01
	0.3		0.4527	87.99	0.81	1.17	9.15	5.03	9.18	5.29	5.16	4.75	0.34
	0.5		0.4521	78.71	0.81	1.14	9.21	5.08	9.18	5.29	5.16	4.77	0.82
O(2)	0.0	2.35	0.4536	59.71	1.03	1.24	9.07	4.76	9.22	5.19	5.18	4.57	
	0.1		0.4545	57.27	1.04	1.19	9.06	4.77	9.29	5.24	5.16	4.55	0.08
	0.2		0.4514	61.06	1.02	1.18	9.06	4.77	9.32	5.99	5.16	4.55	0.07
	0.3		0.4478	65.86	1.00	1.17	9.06	4.77	9.34	6.64	5.15	4.55	0.13
	0.4		0.4420	75.88	0.99	1.16	9.06	4.77	9.36	7.67	5.18	4.55	0.20
O(3)	0.0	2.70	0.4536	57.26	1.08	1.23	9.09	4.73	9.20	5.14	5.11	4.55	
	0.1		0.4526	57.91	1.05	1.19	9.10	4.73	9.22	5.15	5.43	4.56	0.04
	0.2		0.4520	58.41	1.01	1.18	9.10	4.73	9.26	5.16	5.81	4.56	0.09
	0.3		0.4529	58.02	1.00	1.18	9.10	4.73	9.23	5.17	6.30	4.56	0.16
	0.4		0.4502	59.11	0.99	1.16	9.10	4.73	9.32	5.18	6.97	4.56	0.25
O(4)	0.0	1.72	0.4536	78.30	0.95	1.24	9.06	4.88	9.24	5.31	5.22	4.73	
	0.1		0.4539	74.69	0.91	1.22	9.09	4.87	9.23	5.30	5.21	5.01	0.02
	0.2		0.4555	65.43	0.92	1.17	9.07	4.88	9.22	5.30	5.23	5.36	0.05
	0.3		0.4609	54.48	0.91	1.19	9.11	4.87	9.25	5.21	5.15	5.73	0.09
	0.5		0.4590	51.97	0.92	1.14	9.11	4.89	9.20	5.30	5.21	7.14	0.22

two sets of results is nevertheless satisfactory and we expect the cluster approximation to become better as the disorder is increased with the introduction of oxygen vacancies. It should be noted that the narrow peak just below ε_F as found in the FLAPW calculation is not reproduced in our cluster calculations.

Due to the fact that $\approx 20\%$ of the valence electrons lie outside of the muffin-tin sphere, the determination of the Fermi energy ε_F is a difficult problem within the multiple scattering cluster description. Fixing ε_F to its FLAPW value leads in the cluster approach to about the same total *muffin-tin* charge per unit cell for the $\delta=0$ reference compound as in the band-structure calculation (less than 2% deviation). Since most of the interstitial charge arises from the rather extended oxygen p orbitals we can try to mimic the interstitial volume by expanding the O-centered spheres by the appropriate amount. (The different radii in a.u. are: $R_Y=2.7$, $R_{Ba}=3.4$, $R_{Cu(1)}=R_{Cu(2)}=2.0$, $R_{O(1)}=R_{O(2)}=R_{O(3)}=2.875$, and $R_{O(4)}=2.678$.) The resulting *total* charge per unit cell is too low by $\Delta\approx 2.5$ electrons with respect to the band-structure value, and ε_F in the cluster calculation would have to be increased by ≈ 0.4 eV for the difference to vanish. In what follows we shall assume that the FLAPW Fermi energy is the correct one for the stoichiometric system and that this missing charge Δ in our ad hoc construction does not change with δ. This latter condition then provides us with the dependence of the Fermi level on stoichiometry. The corresponding results are summarized in Table I where we also display the DOS at ε_F with respect to the muffin-tin zero and the local charges as a function of δ. (The values for the charges are not weighted with their concentration, and we include for oxygen only the p-like states.) Notice that Δ and the DOS are cluster dependent. It is obvious that for the central site in the cluster the approximate determination of the scattering path operator is better than for other sites.

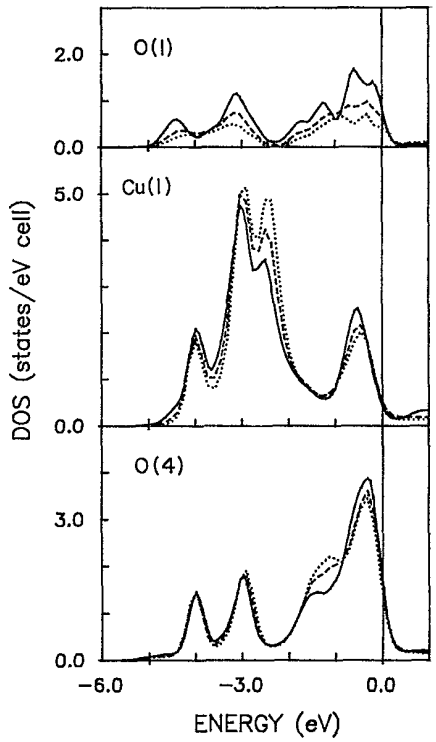

FIG. 2. O(1) and O(4) p-like and Cu(1) d-like DOS for $YBa_2Cu_3O_{7-\delta}$ as a function of the concentration of O(1) vacancies. Solid line: $\delta=0$, dashed line: $\delta=0.3$, and dotted line: $\delta=0.5$.

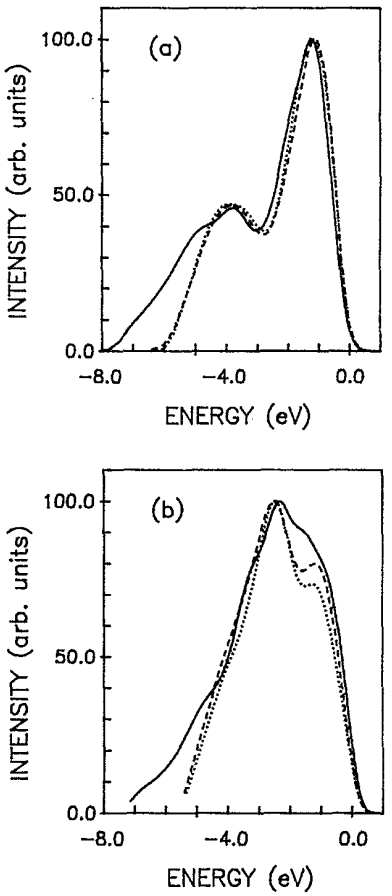

FIG. 3. (a) Calculated O-$K\alpha$ and (b) Cu-L_3 x-ray emission spectra for $YBa_2Cu_3O_{7-\delta}$. Solid line: FLAPW (Ref. 19), dashed line: cluster, $\delta=0$, and dotted line: cluster, $\delta=0.5$.

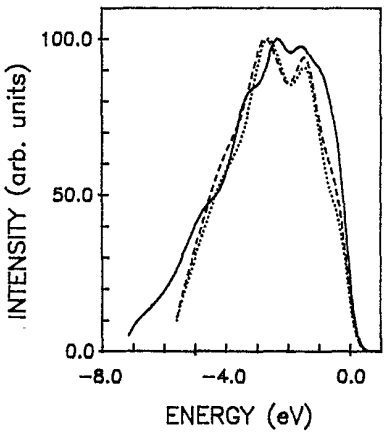

FIG. 4. Theoretical x-ray photoemission spectra for $YBa_2Cu_3O_{7-\delta}$. Solid line: FLAPW (Ref. 19), dashed line: cluster, $\delta=0$, and dotted line: cluster, $\delta=0.5$.

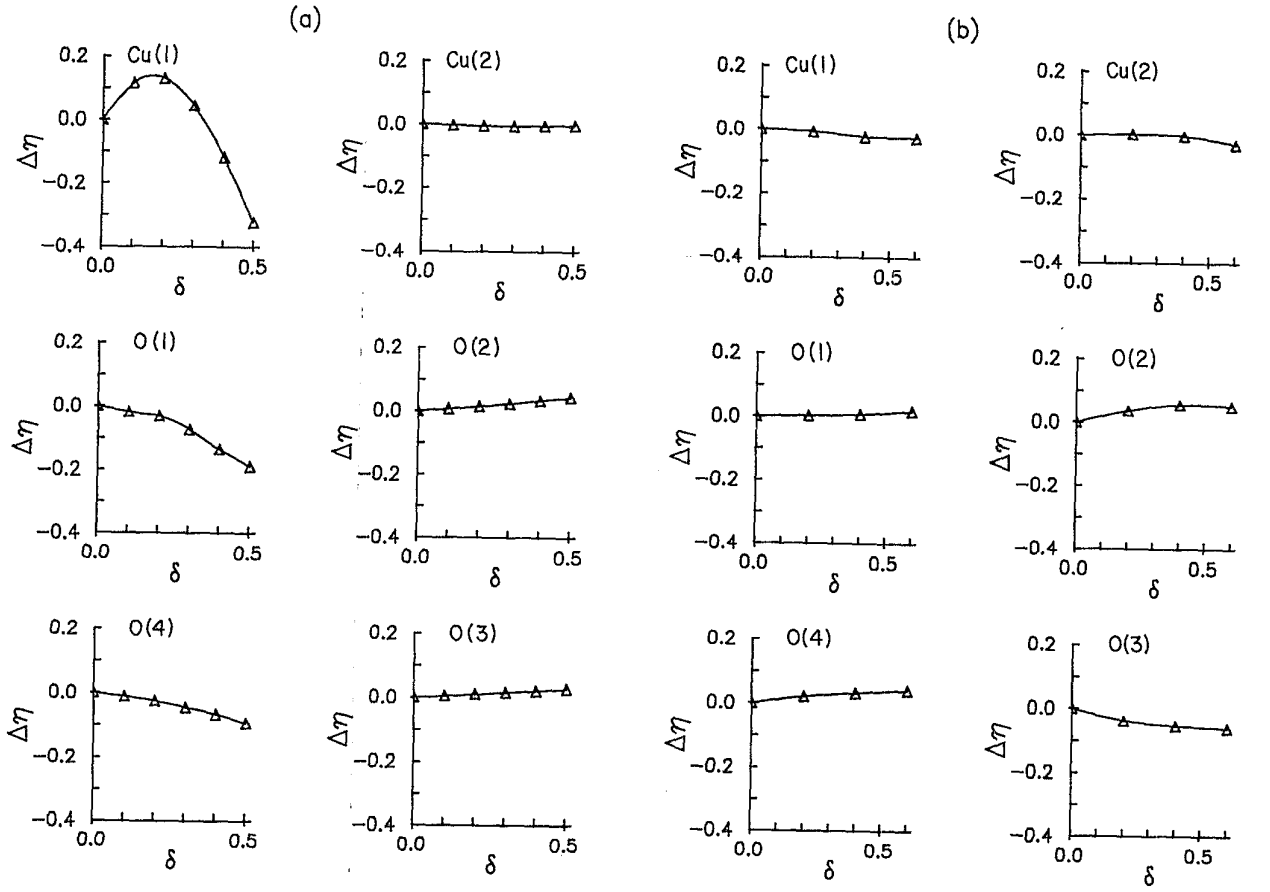

FIG. 5: Calculated deviations of site projected Hopfield parameters (in units eV/Å^2) in $YBa_2Cu_3O_{7-\delta}$ with respect to the stoichiometric ($\delta=0$) case, if (a) vacancies on site O(1) or (b) on site O(2) occur. Solid lines serve as a guide for the eye.

Since at ε_F the partial DOS for O(1), Cu(1), and O(4) are dominant, clusters with these atoms in the center give the best approximation to the band-structure value.

In Table I, we see that the Fermi level ε_F is rather insensitive to δ. As expected, the changes in local charge are limited to the remaining ions on the sublattice on which vacancies are created and to their immediate neighbors. The charge on the ions O(2) to O(4) increases monotonously with the concentration of vacancies on the corresponding sites, due to the polarization of the now asymmetric Cu—O bonds. According to neutron experiments vacancies are preferentially created at the O(1) sites.[16] For this case, we find that the excess charge on the remaining oxygens is much smaller, namely of the same order as on the neighboring Cu(1) ions. The charge in the vacancies is 4 times larger than in the other cases and has a monotonous behavior of δ. We attribute the lower (higher) values of the charge on O(1) (vacancy) to a reduction of the polarizability along the direction of the chain due to the strong Cu(1)—O(4) bond. As seen in Fig. 2, which shows the LDOS at O(1), Cu(1), and O(4) in function of the concentration of O(1) vacancies, part of the charge from the broken Cu(1)—O(1) bonds moves into a nonbonding Cu(1) state at −2.4 eV (labeled *D* in Fig. 4 of Ref. 13. This behavior was already suggested by calculations on very small clusters[17] and is generally observed also in substoichiometric transition-metal carbides and nitrides.[18]

For comparison with experiment, our calculated excitation spectra have been corrected for lifetime effects and finite instrumental resolution as discussed in detail in Ref. 19. As noticed by several authors,[19,20] the theoretical spectra are off by about 2 eV, which merely indicates that the density functional theory does not provide excitation energies. Therefore, we will consider only the relative changes due to the different oxygen concentrations in the calculated spectra.

In Figs. 3(a) and 3(b) we present $OK\alpha$ and CuL_3 XES spectra, respectively. In these figures the FLAPW results (solid line) are compared to the cluster calculations for $\delta=0$ (dashed line) and to one particular substoichiometric case [$\delta=0.5$ for O(1), dotted line]. The peak positions are well reproduced within the cluster approach. In the cluster calculation, however, the main peak in Fig. 3(b) shows a distinct shoulder due to a broader splitting of the two corresponding maxima in the Cu(2) *d*-like LDOS [see Fig. 1(b)]. A finite number of vacancies does not affect the spectra at all. The differences are really marginal and are within the experimental uncertainty as can also be seen from the available experiments.[21] A similar picture pertains for the XPS spectra (Fig. 4), namely that oxygen deficiencies do not result in a detectable shift of the main peak as long as one remains in the orthorhombic phase ($\delta<0.6$).[1]

As last quantity we consider the Hopfield parameter, which describes the electronic contribution to the

electron-phonon coupling constant in the Gyorffy-McMillan formula.[10–12] In Figs. 5(a) and 5(b) we show site projected Hopfield parameters as a function of the concentration of vacancies in the planes and chains, respectively. The strongest dependence is found for $\mu^{Cu(1)}$ with vacancies in the chains, which displays a maximum around $\delta=0.2$. In view of the uncertainty in the deformation of the Fermi level in the cluster approach, we have repeated the calculations for a range of values of ε_F. As expected, the absolute values of the Hopfield parameters change but the relative trends with respect to δ, in particular the maximum of $\mu^{Cu(1)}$ remains. It is an interesting coincidence that the latter is found at the composition at which an abrupt jump in T_c is observed. Note also the steady decrease of $\mu^{O(1)}$ as a function of δ due to the reduced coupling along the chain upon creation of vacancies.

V. SUMMARY

We have presented a real-space cluster formalism which allows a systematic study of the influence of non-stoichiometry on the electronic structure of complex systems. We have applied it to mimic the behavior of bulk $YBa_2Cu_3O_{7-\delta}$ as a function of δ, and find that oxygen vacancies have a rather small effect on the DOS and excitation spectra. This effect is largest for the experimentally observed position [O(1) chain site] of the vacancies but still too small to be detected spectroscopically. Similarly, the dependence of the site projected Hopfield parameters on the concentration of in-plane [O(2)] vacancies is negligible. For O(1) vacancies, $\mu^{Cu(1)}$ shows a definite maximum at $\delta=0.2$, which may be related to the abrupt change in T_c at that composition.

ACKNOWLEDGMENTS

This paper was supported by the Austrian Fonds zur Förderung der wissenschaftlichen Forschung (P7064 and P6835), the Austrian Ministry of Science (Zl. 49.554/1-27a/88), and the Swiss National Science Foundation.

[1] R. Beyers, G. Lim, E. M. Engler, V. Y. Lee, M. L. Ramirez, R. J. Savoy, R. D. Jacowitz, T. M. Show, S. La Placa, R. Boehme, C. C. Tsuei, S. I. Park, M. W. Shafer, and W. J. Gallagher, Appl. Phys. Lett. **51**, 614 (1987); I. K. Schuller, D. G. Hinks, M. A. Beno, D. W. Capone II, L. Soderholm, J.-P. Locquet, Y. Bruynseraede, C. U. Segre, and K. Zhang, Solid State Commun. **63**, 385 (1987).

[2] Y. Tokura, J. B. Torrance, T. C. Huang, and A. I. Nazzal, Phys. Rev. B **38**, 7156 (1988).

[3] B. L. Gyorffy, Phys. Rev. B **5**, 2382 (1972).

[4] J. S. Faulkner and G. M. Stocks, Phys. Rev. B **21**, 3222 (1980).

[5] P. Weinberger, *Electron Scattering Theory for Ordered and Disordered Matter* (Oxford University Press, Oxford, to be published).

[6] P. J. Durham, D. Ghaleb, B. L. Gyorffy, C. F. Hague, J.-M. Mariot, G. M. Stocks, and W. M. Temmerman, J. Phys. F **9**, 1719 (1979).

[7] E. Bauprez, C. F. Hague, J.-M. Mariot, F. Teyssandier, J. Redinger, P. Marksteiner, and P. Weinberger, Phys. Rev. B **34**, 886 (1986).

[8] H. Winter, P. J. Durham, and G. M. Stocks, J. Phys. F **14**, 1047 (1984).

[9] J. Redinger, P. Marksteiner, and P. Weinberger, Z. Phys. B **30**, 321 (1986).

[10] H. Winter, J. Phys. F **11**, 2283 (1981).

[11] G. D. Gaspari and B. L. Gyorffy, Phys. Rev. Lett. **28**, 801 (1972).

[12] W. H. Butler, Phys. Rev. B **15**, 5267 (1977).

[13] S. Massidda, Jaejun Yu, and A. J. Freeman, Phys. Lett. A **122**, 198 (1987).

[14] G. Ginatempo and J. B. Staunton, J. Phys. F **18**, 1827 (1988).

[15] H. Krakauer, W. E. Pickett, and R. E. Cohen, J. Superconduct. **1**, 111 (1988).

[16] A. Santoro, S. Miraglia, F. Beech, S. A. Sunshine, D. W. Murphy, L. F. Schneemeyer, and J. V. Waszczak, Mater. Res. Bull. **22**, 1007 (1987).

[17] H. Eschrig and G. Seifert, Solid State Commun. **64**, 521 (1987).

[18] G. H. Schadler and R. Monnier, Z. Phys. B **76**, 43 (1983); P. Marksteiner, P. Weinberger, A. Neckel, R. Zeller, and P. H. Dederichs, Phys. Rev. B **33**, 812 (1986).

[19] J. Redinger, A. J. Freeman, Jaejun Yu, and S. Massidda, Phys. Lett. A **124**, 469 (1987).

[20] Jaejun Yu, S. Massida, and A. J. Freeman, Phys. Lett. A **122**, 203 (1987).

[21] J. M. Mariot, V. Barnole, C. F. Hague, G. Vetter, and F. Queyroux, Z. Phys. B **75**, 1 (1989).